Visualization of Rotation Fields

Mark A. Livingston

Department of Computer Science
University of North Carolina at Chapel Hill
http://www.cs.unc.edu/~us/rotfield.html

Abstract

We define a *rotation field* by extending the notion of a vector field to rotations. A vector field has a vector as a value at each point of its domain; a rotation field has a rotation as a value at each point of its domain. Rotation fields result from mapping the orientation error of tracking systems. We build upon previous methods for visualization of vector fields, tensor fields, and rotations at a point to visualize a rotation field resulting from calibration of a commonly-used magnetic tracking system.
CR Categories: I.3.3 [Computer Graphics]: Picture/Image Generation; I.3.8 [Computer Graphics]: Applications;
Keywords: Scientific visualization, tufts, streamlines, stream surfaces.

1 Introduction

We define a *rotation field* by building on the common notion of vector fields. We will assume the following informal definition of a vector field.

> A *vector field* maps points in a domain to vectors.

Similarly, we can informally define a rotation field.

> A *rotation field* maps points in a domain to rotations.

Our data comes from mapping the orientation error of a Flock of Birds$^{\mathrm{TM}}$ [Ascension95] magnetic tracking system in our laboratory. In this application, we measure the error in the reported orientation of the sensor relative to the tracking system's reference coordinate frame. Other applications which give rise to rotation fields include visualization of torque in air flow and visualization of molecule-protein interactions.

1.1 Representation of Rotations

In computer graphics, there are three common ways to represent rotations in $\Re^3$: Euler angles, quaternions, and 3×3 orthonormal matrices [Foley90]. Each method has advantages and physical representations that can be exploited in visualization algorithms. Euler angles have the advantage of simplicity of representation. Quaternions use an axis-and-angle parameterization, and this can provide a suitable visualization as well. Matrices can be converted into x-y-z axis tripods for a convenient physical representation.

1.2 Previous Work

1.2.1 Vector field visualization

Recently developed techniques for visualization of vector fields have focused on depicting the field through its action on various types of particles. Streaklines, particle paths, and streamlines [Bryson92] are analogous to tools used in physical wind tunnels for flow visualization. Streamlines have the property of being everywhere tangent to the vector field. Several extensions and variations of streamlines have been developed. Stream polygons [Schroeder91] can represent both translations and rotations caused by the vector field. They are oriented normal to the local vector, travel along a streamline, and undergo changes due to orthogonal vector fields. Stream surfaces [Hultquist92] extend the notion of a streamline to two dimensions by tiling nearby streamlines. Streamballs [Brill94] are centered at the locations of particles, but can merge or split depending on their distances. This enables three-dimensional representation of streamlines and local field properties. Flow volumes [Max93] are the volumetric equivalent of stream lines. They function similarly to the physical technique of dye advection, allowing observers to watch (virtual) smoke pass through the field. A simple and common technique is that of tufts [Bryson92], showing a single vector that is the value of the field at the given location.

1.2.2 Tensor field visualization

Research in tensor field visualization is more recent than in vector field visualization. Ellipsoids [Hesselink94], tensor glyphs [Haber90], and probes [vanWijk94] show the value of the field at a single point. Ellipsoids are stretched along their principal axes according to the field values. Tensor glyphs undergo changes due to the action of the field. A probe is a cylindrical arrow with a base. It can depict convergence, shear, velocity, acceleration, curvature, and rotation. Hyperstreamlines [Delmarcelle94] extend the notion of streamlines to tensor fields. A hyperstreamline is defined as "a geometric primitive having a finite size [swept] along one of the eigenvector fields …while [stretched] in the transverse plane under the combined action of the other two orthogonal eigenvector fields." Thus it builds on the notion of visualizing a field through its action on a primitive object.

1.2.3 Visualization of rotations

Visualization of rotations has also attracted interest. This has proven to be a difficult visualization problem due to the non-linear nature of rotations and the problems of representations of rotations. Orientation maps [Alpern93] use an axis-angle representation of a rotation, scaling the axis in proportion to a function of the angle. (This is similar, but not identical, to a quaternion.) The quaternion demonstrator and the belt trick [Hart94] show how the quaternion acts

through a series of turns, in order to understand how quaternions relate to rotations. The Dirac string trick [Francis94] functions similarly. Quaternion frames [Hanson94] can represent space curves. The frames can then be represented on the sphere or visualized with 4D lighting techniques. Spherical color maps [Yamrom94] assign a color to each orientation, then color the domain over which the orientations occur with these colors.

1.3 Driving Problem

Previous methods do not necessarily extend well to rotation fields or provide suitable visualizations for our application. Our driving problem is the visualization of orientation error from a Flock of Birds magnetic tracking system. We measure the error [Livingston97] at a series of irregularly distributed points by using a Faro Technologies Metrecom IND-01 mechanical tracking system [Faro93] as a reference. We then resample the error into a regular grid over the three translational dimensions relative to the transmitter of the tracker. The resampling uses a Gaussian kernel at each desired grid point and computes a weighted average of the samples within a user-controlled distance. We express the error as a rotation at the measured points and at the grid points.

We need to identify regions of the field in which the measured (or resampled) rotations differ from nearby rotations (heterogeneity). This difference could be seen in either the axis of rotations or in the magnitude of the rotation, or both. We also need to identify regions in which the magnitude of the error is greater than a tolerance. The former can imply poor sampling frequency, while the latter can reveal the presence of hidden sources of distortion of the magnetic field. Consequently, we must be able to relate the visualization to the physical space represented. The transmitter of the tracking system defines a global coordinate system for this space. We measure orientation error as deviation from this global system.

Vector representations (such as mapping Euler angles to Cartesian axes or using the axis of the quaternion) fail to adequately capture all of the information of a rotation field. While a rotation field has similarities to tensor fields (e.g. significance of eigenvectors), it is not strictly a tensor field, since it is non-linear and the dependent variables (the three degrees of freedom of the rotations) are not independent. However, the techniques described above for tensor fields can be applied. Due to the density of the field and our need to understand its heterogeneity, we found the ellipsoid and tensor glyphs insufficient for detailed analysis of the rotation field. Hyperstreamlines appear to be suitable, and if anything offer too much flexibility, plus the shaded polyhedral shapes can be expensive to render. The same limitations apply to visualization of rotation fields with probes.

2 Visualization Methods

We introduce four visualizations of rotation fields. Two are point icons, one is a line icon similar to hyperstreamlines, and one is a surface icon similar to hyperstreamlines and stream surfaces. Drawing on the work in animated visualizations [Ma92][vanWijk94][Yamrom95], we animate all visualizations.

2.1 Cylindrical tufts

We use a triangular cylinder with red, green, and blue sides to create a tuft for rotation. This cylindrical tuft is defined in a local coordinate system, then a copy is translated to the position of each sample. We rotate the cylinder according to the field value to show the effect of the field. The tuft is then oriented around its axis by the angle of rotation. We had hoped this would highlight subtle variations in the field, but it did not. The length of the cylinder can be adjusted to user preference. While this visualization does produce a clear visualization of the field of axes of the respective rotations, it does not highlight subtle differences in the field. To visualize these differences, we animate the tufts by spinning them around their respective axes at speeds proportional to their respective angles of rotation; thus we are animating the second rotation described above. Each tuft makes one complete revolution at its respective speed. The waves of color that emerge from this animation (Plate 1) make apparent even subtle differences at adjacent points of the field. The disadvantage of this method is that the display can become cluttered. Providing depth cues with atmospheric effects improves the visualization slightly.

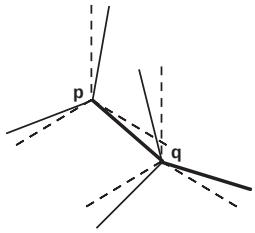

Figure 1: CONSTRUCTING AXIS STREAMLINES. At a point p, the field value is read, producing a rotated axis tripod (solid lines) from the global coordinate system (dashed lines). We take a step along the desired tripod leg (thick line) to arrive at the next point q, from which the integration continues.

2.2 Axis tripods

For a less bulky point icon, we display the local axis tripod, rotated relative to the transmitter's orientation. Plate 2 shows a subset of the tripods located at the sample points. As with the cylindrical tufts, it is difficult to pick out subtle differences in the field. We improve the visualization by warping the axis tripods between the identity rotation and field value. By sampling on a regular 3D grid and choosing appropriate scale factors, the axis tripods can form a 3D grid when all values are warped to the identity rotation. Although the display can quickly become cluttered, we found this visualization useful for locating heterogeneity in the field. Depth cues again reduce the apparent clutter.

2.3 Axis streamlines

In an effort to produce a visualization with less clutter, we drew upon the concept of streamlines. In contrast to hyperstreamlines, we do not want to integrate along the eigenvector of the rotation. We find the eigenvector a non-intuitive visualization. Instead, we introduce *axis streamlines* by integrating along the rotated local x, y, and z vectors associated with the rotation. (A matrix representation of the rotation is quite suitable for computing these vectors efficiently.) These lines are straight lines in the distorted magnetic field of the tracker.

An axis streamline is thus constructed as follows (Figure 1). First, a seed point is chosen. We had a rectangular volume over which we needed to analyze tracker performance, and this provided convenient planes in which to place arrays of seed points. Next, we interpolate the field value from the resampled regular grid using a series of spherical linear interpolations [Shoemake85] to determine the rotation at the current point from the eight surrounding grid points. We apply this rotation and take a step of predetermined length in the rotated x (or y or z) direction. At this new point, the field value is again interpolated and a new step taken. We used a precomputed number of segments to stop the integration, though a physically meaningful stopping criteria would also be suitable (such as leaving the volume of interest in our application).

Axis streamlines reduce the clutter of the display while preserving properties of the data (Plate 3). Depth cues again help reduce the apparent clutter. Using small integration steps enhances features in the data. It can be easy to lose track of the reference frame. Thus we animate the streamlines by warping between straight lines (the identity rotations) and the integrated streamlines. As the lengths of the streamlines grow, the lines can diverge in heterogeneous regions, providing less information in those regions.

2.4 Axis stream surfaces

We can tile between adjacent axis streamlines to create *axis stream surfaces* (Plate 4). Currently we use exactly those axis streamlines produced as described in Section 2.3, with the same seed points. We represent the axis stream surfaces as quadrilateral strips, with one quadrilateral for every step taken beyond the seed point. We animate axis stream surfaces by again warping, as for axis streamlines, between the straight lines and the integrated streamlines. The tiling remains the same between frames; only the positions of the vertices change. Twisting and shearing of axis stream surfaces denote heterogeneity in the field. This is a much easier feature to detect for a surface than for a line. Depth cues improve the visualization somewhat.

3 Results

We found all four visualizations useful for locating heterogeneities in the rotation field, though axis stream surfaces are best. Heterogeneity of the field was crucial information in our analysis of the magnetic tracker performance and the development of our correction method [Livingston97]. That method uses the resampled (regular) grid of translation and rotation error as a lookup table. The lookup table we used was three-dimensional in its input and six-dimensional in its output. The input dimensions correspond to the x, y, and z axes of the tracking system. The output is a translation and a rotation to apply to a reading taken at the given position. We had assumed that this was the appropriate parameter set. (We visualize only the rotation portion of the output in this work.)

The visualizations presented here were not ready in time for use in that work, but we can see with these visualizations that the rotation field exhibits heterogeneity throughout. This reveals poor sampling of the rotation field. With these visualizations, we would have tested our assumption about the parameter set much sooner than we did. When we did test the assumption [Livingston97], we discovered that the rotation field associated with the magnetic tracker needs six input dimensions: the three corresponding to the position of the sensor with respect to the transmitter, and the three corresponding to the orientation of the sensor with respect to the transmitter.

We can also quickly pick out areas in which the error of the tracker is large. The axis streamlines are well-suited to showing this information. This led us to examine the environment more carefully for sources of distortion in the tracker's magnetic field, which is the primary cause of tracker error. These sources may be hidden from view or believed to be benign, but the axis streamlines and axis stream surfaces have shown us regions of the field with high error.

4 Future Work

We hope to create visualization methods that clutter the display even less. We can subsample the field as necessary, but this reduces the information content of the display as well as the visual content. Streamlines depend heavily on the seed placement. Interactive placement would allow the user to control the visualization better; automated placement [Turk96] would also serve us well. Transparency and improved depth cues might enable us to see through axis stream surfaces to the entire field. Extension to volumes would then be an option. We use animation to depict information in the field, but we may need to use animation for display of dynamic data. To visualize our magnetic tracker error data, we need a 6D domain and 6D range visualization method.

Finally, we look forward to applying these methods to new tracking devices and different applications. The data that we have thus far visualized come from data sets with which we have long worked; thus we knew what to expect and needed only to analyze the performance of the visualization methods. New data would challenge our methods to provide insights to unknown fields as well.

5 Acknowledgements

I thank those who contributed ideas, comments, analysis, or time: Greg Turk, Gentaro Hirota, Henry Fuchs, Mary C. Whitton, Andrei State, Hans Weber, Daniel G. Aliaga, Carl Mueller, and Todd E. Gaul. This work was supported in part by ARPA (ISTO DABT-63-93-C-0048) and NSF (ASC-8920219). Approved by ARPA for Public Release - Distribution Unlimited.

References

[Alpern93] Bowen Alpern, Larry Carter, Matt Grayson, and Chris Pelkie. Orientation Maps: Techniques for Visualizing Rotations (A Consumer's Guide). In *IEEE Visualization '93*, pages 183–188, October 1993.

[Ascension95] Ascension Technology Corporation, Burlington, VT. *The Flock of Birds Installation and Operation Guide*, January 1995.

[Brill94] Manfred Brill, Hans Hagen, Hans-Christian Rodrian, Wladimir Djatschin, and Stanislav V. Klimenko. Streamball Techniques for Flow Visualization. In *IEEE Visualization '94*, pages 225–231, October 1994.

[Bryson92] Steve Bryson and Creon Levit. The Virtual Wind Tunnel. *IEEE Computer Graphics and Applications*, 12(4):25–34, July 1992.

[Delmarcelle94] Thierry Delmarcelle and Lambertus Hesselink. Visualization of Second Order Tensor Fields and Matrix Data. In *IEEE Visualization '94*, pages 316–323, October 1994.

[Faro93] Faro Technologies, Incorporated, Lake Mary, FL. *Industrial Metrecom Manual, v2.0*, 1993.

[Francis94] George K. Francis and Louis H. Kauffman. Air on the Dirac Strings. *Comtemporary Mathematics*, 169:261–276, 1994.

[Foley90] James Foley, Andries van Dam, Steven Feiner, and John Hughes. *Computer Graphics: Principles and Practice*, pages 213–217, 1063. Addison-Wesley Publishing Company, 2nd edition, 1990.

[Hesselink94] Lambertus Hesselink and Thierry Delmarcelle. *Scientific Visualization: Advances and Challenges*, chapter 26, pages 419–433. Academic Press in association with IEEE Computer Society Press, 1994.

[Hart94] John C. Hart, George K. Francis, and Louis H. Kauffman. Visualizing Quaternion Rotation. *ACM Transactions on Graphics*, 13(3):256–276, July 1994.

[Haber90] Robert B. Haber and David A. McNabb. Visualization Idioms: A Conceptual Model for Scientific Visualization Systems. *Visualization in scientific computing*, pages 74–93, 1990.

[Hanson94] Andrew J. Hanson and Hui Ma. Visualizing Flow with Quaternion Frames. In *IEEE Visualization '94*, pages 108–115, October 1994.

[Hultquist92] Jeff P. M. Hultquist. Constructing Stream Surfaces in Steady 3D Vector Fields. In *IEEE Visualization '92*, pages 171–178, 1992.

[Livingston97] Mark A. Livingston and Andrei State. Magnetic Tracker Calibration for Improved Augmented Reality Registration. *Presence: Teleoperators and Virtual Environments*, 1997. To appear.

[Max93] Nelson Max, Barry Becker, and Roger Crawfis. Flow Volumes for Interactive Vector Field Visualization. In *IEEE Visualization '93*, pages 19–24, October 1993.

[Ma92] Kwan-Liu Ma and Philip J. Smith. Virtual Smoke: An Interactive 3D Flow Visualization Technique. In *IEEE Visualization '92*, pages 46–53, 1992.

[Shoemake85] Ken Shoemake. Animating Rotation with Quaternion Curves. In *Computer Graphics (SIGGRAPH '85 Proceedings)*, volume 19, pages 245–254, July 1985.

[Schroeder91] William Schroeder, C. R. Volpe, and W. E. Lorensen. The Stream Polygon: A Technique for 3D Vector Field Visualization. In *IEEE Visualization '91*, pages 126–132, 1991.

[Turk96] Greg Turk and David Banks. Image-guided Streamline Placement. In *SIGGRAPH 96 Conference Proceedings*, Annual Conference Series, pages 453–460. ACM SIGGRAPH, Addison Wesley, August 1996.

[vanWijk94] Jarke J. van Wijk, Andrea J.S. Hin, Willem C. de Leeuw, and Frits H. Post. Three Ways to Show 3D Fluid Flow. *IEEE Computer Graphics and Applications*, 14(5):33–39, September 1994.

[Yamrom95] Boris Yamrom and Kenneth M. Martin. Vector Field Animation with Texture Maps. *IEEE Computer Graphics and Applications*, 15(2):22–24, March 1995.

[Yamrom94] Boris Yamrom, John A. Sutliff, and Andrew P. Woodfield. Visualizing Polycrystalline Orientation Microstructures with Spherical Color Maps. In *IEEE Visualization '94*, pages 46–51, October 1994.

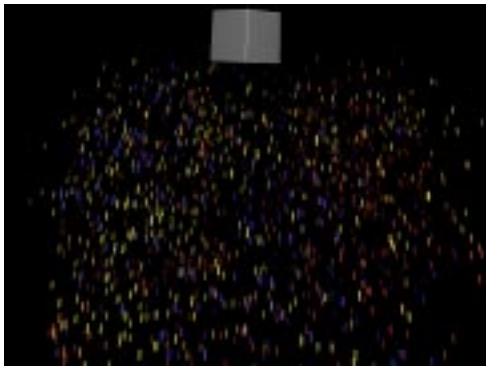

Plate 1: CYLINDRICAL TUFTS. Waves of color produced by spinning the tufts at rates proportional to the angle of the rotation enhance the visualization of subtle changes in adjacent measurements. The gray box at the top (in this and other plates) represents the transmitter of the magnetic tracking system.

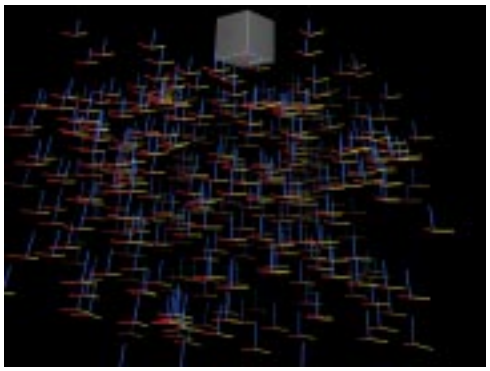

Plate 2: AXIS TRIPODS. Each tripod is rotated with respect to the global coordinate system by the field value at that point.

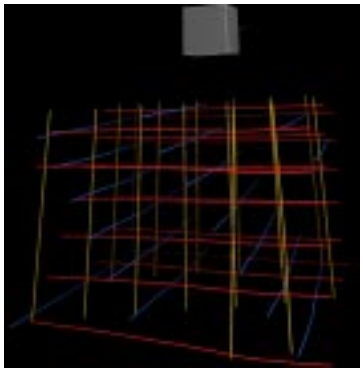

Plate 3: AXIS STREAMLINES. Integration over a series of axis tripods produces streamlines of the rotated local x, y, and z coordinate axes.

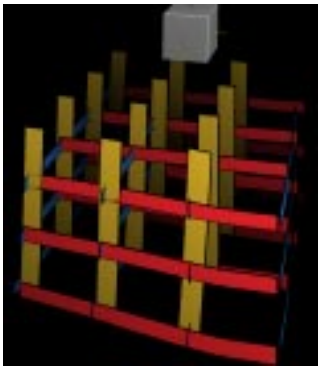

Plate 4: AXIS STREAM SURFACES. Tiling axis streamlines to produce axis stream surfaces enhances the visualization.